The relationships between absorbing aerosols and snow cover/snow water equivalent over the Himalayas and the western Tibetan Plateau during boreal spring.

Woo-Seop Lee[1], Maeng-Ki Kim[1], KM Lau[2], Kyu-Myong Kim[3] and Sung Kim[1]

[1] Department of Atmospheric Sciences, Kongju National University, Gongju, 314-701, Korea
[2] Laboratory of Atmospheres, NASA Goddard Space Flight Center, Greenbelt, MD 20771, USA
[3] Goddard Earth Sciences and Technology Center, University of Maryland Baltimore County, Baltimore, MD 21228, USA

1. Introduction

Many factors besides greenhouse warming could have led to accelerated warming over the Himalayas and TP. These include increased land-use and land change, increased sunlight duration from reduction in cloudiness, increased water vapor feedback, and reduction of snow albedo by deposition of soot and dust on snow surface (Kang *et al* 2000, Prasad and Singh 2007, Flanner *et al* 2007, 2009, Yasunari *et al* 2009). Recently Ramanathan *et al* (2007) estimated that atmospheric heating by Asian Brown Clouds (ABC) double the greenhouse warming over South Asia, and may contribute substantially to the loss of glacier mass in the Himalayas. In contemporary papers, Lau *et al* (2006), Lau and Kim (2006) and Lau *et al* (2008) proposed the "elevated heat pump" (EHP) mechanism by which absorbing aerosols may affect on the South Asian monsoon. They demonstrated that du and black carbon transported to high-altitude in the Himalayas and TP region in boreal spring can induce upper tropospheric heating over the TP through atmospheric feedback processes, leading to enhanced rainfall in the Himalayas foothills in the late spring and early summer. Long-term upper tropospheric warming consistent with the EHP hypothesis over the western Himalayas has been observed (Gautam *et al* 2009, Prasad *et al* 2009).

In this study ,we will investigate the impact of atmospheric heating by dust and black carbon in possibly leading to enhanced pre-summer monsoon surface warming and early sno melt in the Himalayas and TP region. The snow-darkening effect by black carbon and dust is not considered in the present study.

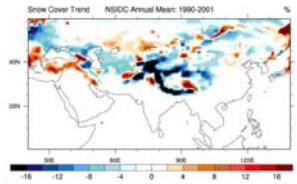

Fig. 5. Trend in annual linear snow cover (% per decade) from 1990 to 2001 as obtained from the National Snow and Ice Data Center (NSIDC) EASE-Grid weekly snow cover and sea ice extent dataset (Armstrong and Brodzik, 2005). Trend is based on a least-square linear fit.

2. Model Experiments

- **NASA fvGCM (Lin, 1997; Lin and Rood, 1996, 1997)**
- The fvGCM has a 2 x 2.5 degree resolution, 55 layers in the vertical and is coupled to the NCAR community land model (Dai *et al* 2002) and a perturbation mixed layer ocean (MLO) model. (Waliser *et al* 1999).
- McRAS (Sud and Walker,1999)
- Radiative transfer model (Chou and Suarez, 1999; Chou et al., 2001)
- Land surface model (Bonan, 1996), PBL (Holtsage and Boville, 1992)
- Global aerosol loading
- Is prescribed from monthly climatologies (interpolated to daily values) of four-dimensional distributions of each of the five aerosol species (dust, black carbon, organic carbon, sulfate, and sea salt) derived from the Goddard Chemistry Aerosol Radiation Transport (GOCART) model (Chin *et al* 2002, 2004).
- Both shortwave and longwave forcing are included.

- Model experiments.

- Control experiment: No aerosol experiment (**NA**) with the prescribed weekly SST
- Aerosol experiments:
  ; The same as NA except for one with the aerosol radiative forcing for five **aerosols species (dust, black carbon, organic carbon, sulfate, and sea salt)**
- Aerosol forcing: 3D-monthly AOT of the five aerosols by GOCART model (Chin et al., 2003)
- Model run period: 01/04/2000– 31/10/2007 (8 years)
- two sets of 4-member ensemble experiments with different initial conditions have been carried out

3. Result

a. Warming over the TP and the EHP Effect

Table 1. Mean aerosol optical depth (AOD) and the percentage contributions from each of five aerosol species used in this study averaged over Indo-Gangetic Plane (IGP), Tibetan Plateau (TP), and the Central China, for the month of May. MODIS AOD is undefined over the TP.

	IGP [25~30°N, 75~85°E]	Tibetan Plateau [30~35°N, 80~95°E]	Central China [25~35°N, 105~120°E]
GOCART	0.41	0.14	0.73
MODIS	0.65	-	0.61
Black Carbon	11.6%	10.4%	8.0%
Dust	45.2%	44.4%	16.8%
Sulfate	16.7%	22.2%	62.0%
Organic Carbon	24.1%	19.4%	12.3%
Sea salt	2.5%	2.1%	1.0%

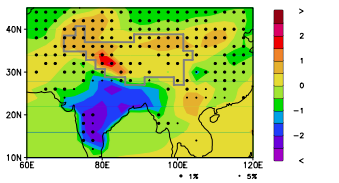

Figure 2. Spatial distribution of simulated difference of surface skin temperature(℃) between AA and NA runs for May. Grid points with statistical confidence level exceeding 5% and 1% are indicated by small and large close circles.

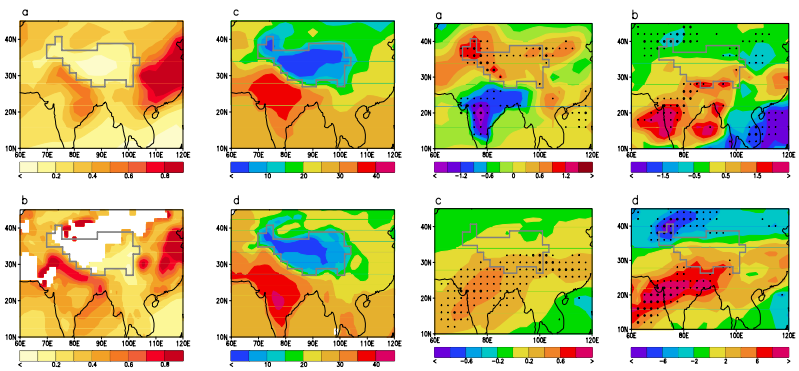

Figure 1. Spatial distribution of aerosol optical thickness (AOD) by (a) GOCART and (b) MODIS observation (2000 to 2009), (c) air temperature in NA run and (d) for observation (AIRS, 2003 to 2009) for May

Figure 3. Spatial patterns of (a) 2m air temperature(℃), (b) precipitation(mm/day), (c) layer mean specific humidity between 700hPa and 300hPa (g/kg), and (d) total cloud cover (%) differences `defined as the monthly mean difference between AA and NA runs for May. Gray line outlines the boundary of Tibetan Plateau. Grid points with statistical confidence level exceeding 5% and 1% are indicated by small and large close circles.

b. EHP-induced snowmelt, and changes in surface energy balance

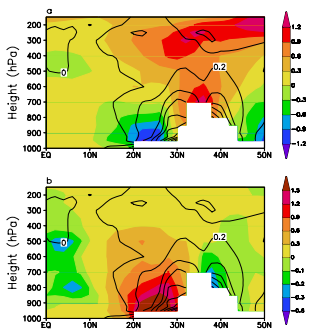

Figure 4. Latitude-height cross-section of the simulated difference (AA-NA) of the shortwave radiative forcing (shaded, ℃/day) and (a) temperature (℃) and (b) specific humidity (g/Kg) averaged between 70 and 100E for May. The model profile of the Tibetan Plateau is indicated by the white shading

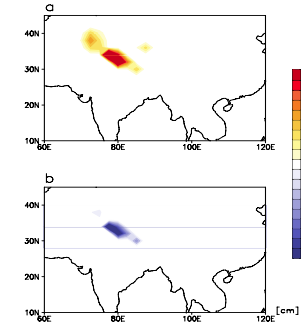

Figure 5. Spatial distribution of (a) mean climatology of April–May snow depth from the control experiment and (b) snow depth change (cm) induced by aerosols (AA minus NA).

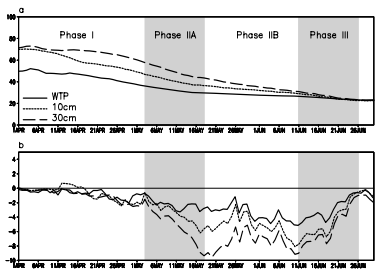

Table 2. Area mean snow depth anomalies, defined as monthly mean difference between AA and NA runs, over the Tibetan Plateau (TP), the western TP, and the eastern TP. Climatological mean values of snow depth from the control experiment are shown in parentheses. The western and eastern TP are defined with respect to 90E longitude line. Units are in cm. Bold face types indicate statistically significant at least 5% level. (*) indicates values significant at 1% level.

	Tibetan Plateau	W. Tibetan Plateau	E. Tibetan Plateau
April	-0.81 (33.82)	-1.27 (62.12)	-0.05 (0.81)
May	-2.24* (13.22)	-3.63* (24.47)	-0.01 (0.09)
June	-0.73* (2.03)	-1.18* (3.76)	-0.00 (0.01)

Figure 6. Time variation of a) area mean climatological surface albedo (%) in NA run, and b) relative percentage change of surface albedo (%) in AA run as compared to NA run over the western Tibetan Plateau (WTP, solid line). Dotted and dashed lines are albedo changes from the region where the climatological snow depths are larger than equal to 10 cm (dotted line) or 30cm (dashed line), respectively.

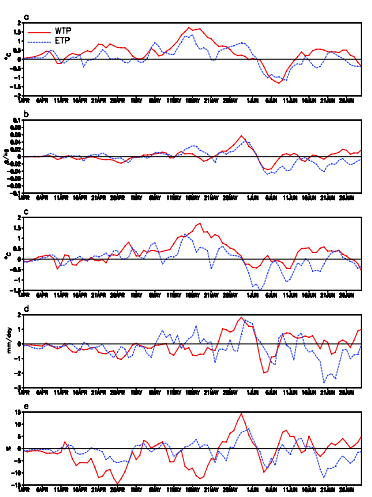

Figure 6. Time series of AA-minus-NA daily mean of (a) surface air temperature (℃), (b) surface skin temperature (℃), (c) specific humidity (g/kg) in upper troposphere between 700 and 300hPa, (d) precipitation (mm/day), and (e) total cloud fraction (%) over the western Tibetan Plateau (solid line) and the eastern Tibetan Plateau (dotted line).

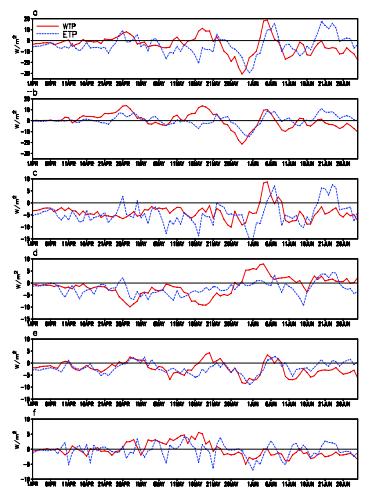

Figure 7. Time series of AA minus NA daily mean of (a) net shortwave, (b) net longwave, (c) net radiative fluxes, (d) latent heat flux, (e) sensible hear flux, and (f) net surface flux at surface over the western Tibetan Plateau (solid line) and the eastern Tibetan Plateau (dotted line). Units are W/m². Positive flux indicates downward for shortwave (a), net radiative (c), and net heat fluxes (f) while positive flux indicates upward for longwave (b), latent (d) and sensible (e) fluxes.

4. Conclusion

From numerical experiments with the NASA fvGCM , we found that the heating of the troposphere by elevated dust and black carbon aerosols in the boreal spring can lead to widespread enhanced warming of the land-atmosphere, and accelerated snow melt in the Himalayas and Tibetan region. The warming and snowmelt are most pronounced in the western Tibetan Plateau region in late April to mid-May, where the climatological snow cover is deeper and more extensive compared to the eastern Tibetan Plateau. The surface shortwave and longwave radiative fluxes are closely linked to the variations of cloudiness, and largely offsetting each other, with an overall net cooling effect. The surface heating and accelerated snowmelt stem from an effective transfers heat from atmosphere to land through sensible and latent heat fluxes (~5-10 Wm^{-2}), outweighing the net radiative (SW + LW) cooling effect (< 5 Wm^{-2}).

Climatologically, during boreal spring, the surface of Tibetan Plateau is heated by increased seasonal solar radiation, and the atmosphere over the Plateau by sensible heat flux, and to a lesser degree by latent heat flux (Yanai and Wu 1990, Yanai *et al* 1992). Our results suggest that as a response to radiative forcing by dust and black carbon in the Indo-Gangetic Plain and Himalaya foothills, the atmosphere over the Plateau is anomalously heated, and moistened via the EHP effect (Lau *et al* 2006). The warm and moist atmosphere overlying the TP land surface, causes a reduction in surface sensible and latent heat fluxes from land to atmosphere, *i.e.*, a net heat gain by the land surface. The net heat gained is used for melting more snow over the TP and the Himalayas. Effectively, the anomalous atmosphere heat energy induced by solar heating of aerosols is transfer from atmosphere to land to enhance the seasonal warming of the land surface and the melting of snow in the region.